

## A METHOD FOR COAL STRUCTURE DIVISION BASED ON AVO SIMULTANEOUS INVERSION

HAIBO WU, SHOUHUA DONG, YAPING HUANG, GUIWU CHEN and HAOLONG WANG

*School of Resources and Geosciences, China University of Mining and Technology, Xuzhou, P.R. China. zywt@cumt.edu.cn, wuhaibocumt@163.com*

(Received November 19, 2014; revised version accepted June 17, 2015)

### ABSTRACT

Wu, H., Dong, S., Huang, Y., Chen, G. and Wang, H., 2015. A method for coal structure division based on AVO simultaneous inversion. *Journal of Seismic Exploration*, 24: 365-378.

Prospecting for enriched areas must be the primary goal of seismic exploration of coal-bed methane (CBM) reservoirs, and coal structure is the principal factor controlling CBM enrichment within a mining field that has relatively uniform geological characteristics such as reservoir thickness, cap rock, and coal quality. Based on reservoir rock physics and coal structure theory, this study found that development areas of mylonitized coal, which correspond to CBM-enriched areas, show abnormally low values of P-wave and S-wave impedance ( $I_p$  and  $I_s$ ). It was also established that  $I_p$  and  $I_s$  act as valid parameters for coal structure division. Before adopting a pre-stack inversion for  $I_p$  and  $I_s$ , the applicability of the AVO approximation equation (expressed by  $I_p$  and  $I_s$ ) with small incidence angles ( $< 30^\circ$ ) was tested and verified. Thereafter, the AVO inversion equation based on Bayes' theorem could be derived by adopting the modified Cauchy distribution as the prior distribution. A test using a model typical of a CBM reservoir containing Gaussian white noise illustrated the stability of this inversion method and provided accurate inversion values for  $I_p$  and  $I_s$ . Moreover, the seismic profile of a CBM reservoir in a field in Qinshui Basin, as an inversion case study, revealed an area of abnormally low values of  $I_p$  and  $I_s$ . This demonstrated that the method is capable of the effective division of coal structure types in a CBM reservoir and of the delineation of areas of mylonitized coal development.

**KEY WORDS:** CBM-enriched area, coal structure, Bayes' theorem, AVO simultaneous inversion, impedance, mylonitized coal.

## INTRODUCTION

Coal-bed methane (CBM) as an unconventional energy source could significantly contribute to the energy for industrial production. However, CBM enrichment also has serious implications on mine safety. Accordingly, prospecting for CBM-enriched areas must be the primary goal of exploration, but with the adoption of applied exploration and exploitation techniques (Qi and Zhang, 2012). Other than conventional gas (C-Gas), most CBM is absorbed and enriched on the surface of the coal matrix (Fu et al., 2007). Therefore, it is crucial to evaluate the degree of enrichment of a CBM reservoir using geophysical means, even though the degree of CBM enrichment causes complicated changes in the elastic parameters of the reservoir (Chen et al., 2014).

Some geophysical experts have attempted to make qualitative evaluations of CBM-enriched areas based on factors that control CBM enrichment such as coal structure. Wang (2012) attempted the division of a CBM outburst zone by regarding the thickness of the tectonic coal as the principal weighting factor of CBM enrichment. Li et al. (2013) determined development areas of CBM reservoir tectonic coal and estimated the level of danger of a CBM outburst based on elastic impedance data as well as on the post-stack inversion results. Peng et al. (2005, 2006) exploited the AVO attribute inversion to indicate the degree of fracture development within different coal structure types, based on which they predicted CBM-enriched areas. In addition, Chen et al. (2013, 2014) discussed the differences in the physical characteristics of rock between CBM and C-Gas, and analyzed the correlation between gas content and elastic parameters using statistical data. Overall, there has been less research on the seismic exploration of CBM-enriched areas and little research on the geological characteristics and rock physics of CBM reservoirs.

Compared with a post-stack inversion, a pre-stack AVO inversion can provide greater quantities of information about reservoir rock physics and pore fluid. Buland and Omre (2003) proposed using the Bayesian linearized AVO inversion and conducted a three-parameter AVO inversion. Downton (2005) analyzed the errors within a pre-stack inversion and performed an AVO waveform inversion based on Bayes' theorem. Alemie (2010, 2011) selected a trivariate Cauchy distribution as the prior distribution to enhance the precision of an AVO inversion. A probabilized pre-stack AVO inversion based on Bayes' theorem has become commonplace and therefore, in this paper, values of P-wave and S-wave impedance ( $I_p$  and  $I_s$ ) and  $\rho$  of a CBM reservoir were obtained by drawing support from an AVO simultaneous inversion based on Bayes' theorem and using reservoir rock physics and coal structure types as a theoretical basis. By applying  $I_p$  and  $I_s$  data, the division of coal structure types was realized, especially the delineation of areas of mylonitized coal development, indicating the possibility of further division of CBM-enriched areas.

ROCK PHYSICS BASIS AND COAL STRUCTURE TYPES OF CBM RESERVOIR

As the occurrence locus of CBM, the physical properties of a coal reservoir’s rock (especially pore-fracture characteristics) seriously affect CBM enrichment. Coal structure is the principal factor controlling CBM enrichment within a mining field that has relatively uniform geological characteristics such as reservoir thickness, cap rock, and coal quality. Fig. 1 exhibits the typical parameters of rock physics of coals with different coal structure types.

Generally, coal structure is classified into one of three types: primary coal, fragmented coal, and mylonitized coal, as shown in Fig. 1. CBM enrichment is enhanced by the degree of crushing of the coal structure. Mylonitized coal has a highly crushed structure and the developmental pores present favorable areas for CBM adsorption, whereas primary and fragmented coal have limited developmental bedding and the cracks represent areas suitable for CBM transfusion (Fu et al., 2007). As shown in Fig. 1, the rock physics parameters, especially  $I_p$  and  $I_s$  of mylonitized coal are obviously less than those of primary and fragmented coal. Therefore, obtaining impedance parameters ( $I_p$  and  $I_s$ ) by applying seismic data inversion could be an efficient method for distinguishing coal structure types and delineating areas of mylonitized coal development.

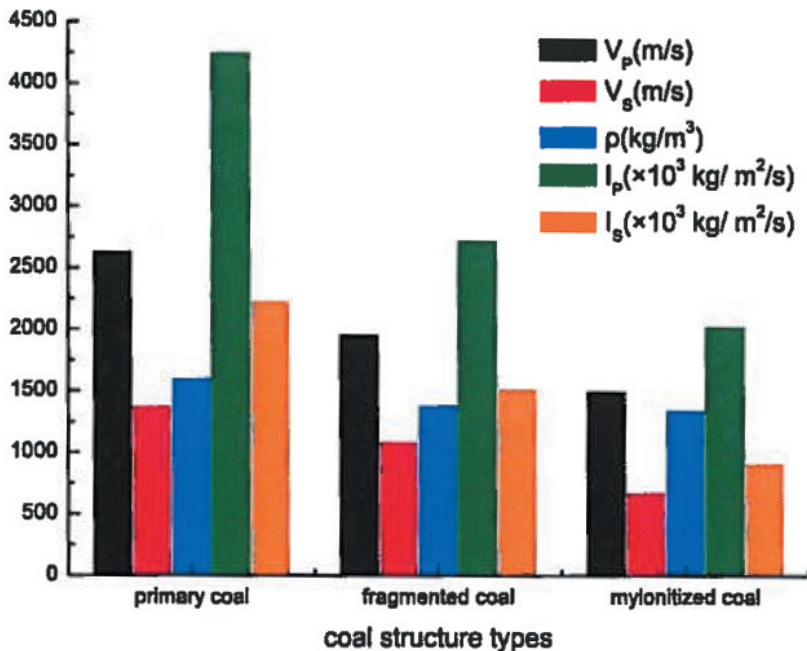


Fig. 1. Typical rock physics parameters of coals with different structure types.

## AVO SIMULTANEOUS INVERSION BASED ON BAYES' THEOREM

### AVO approximation equation of Zoeppritz and its applicability

Pre-stack seismic data have abundant rock physics information. Through an AVO simultaneous inversion, it is possible to obtain details of the parameters of reservoir rock physics such as velocity, density, impedance parameters, Young's modulus, and the Poisson ratio. However, most inversion work is completed with the aid of AVO approximation equations because of the strong nonlinearity of the Zoeppritz equation (Ma and Geng, 2013). An approximation equation expressed by  $I_p$  and  $I_s$  has better stability and eq. (1) is derived from Fatti et al. (1994):

$$R_{pp}(\theta) = \frac{1}{2}(1 + \tan^2\theta)(\Delta I_p/I_p) - 4(V_s/V_p)^2 \sin^2\theta(\Delta I_s/I_s) - [\frac{1}{2}\tan^2\theta - 2(V_s/V_p)^2 \sin^2\theta](\Delta\rho/\rho) \quad (1)$$

where  $V_p$  and  $V_s$  are the P-wave and S-wave velocity of the medium, respectively,  $\rho$  is the density,  $\theta$  is the average value of the incidence angle and transmission angle, and they must satisfy the following equations:

$$\begin{aligned} I_p &= (\rho_1 V_{p1} + \rho_2 V_{p2})/2, \quad \Delta I_p = (\rho_2 V_{p2} - \rho_1 V_{p1}) \quad , \\ I_s &= (\rho_1 V_{s1} + \rho_2 V_{s2})/2, \quad \Delta I_s = (\rho_2 V_{s2} - \rho_1 V_{s1}) \quad , \\ \rho &= (\rho_1 + \rho_2)/2, \quad \Delta\rho = (\rho_2 - \rho_1), \quad \text{and } \theta = (\theta_1 + \theta_2)/2 \quad , \end{aligned}$$

where subscripts 1 and 2 indicate the upper and lower media.

The basic assumption of the approximation equation is that the elastic parameters of the media on both sides of the reflection interface are similar. However, large differences do exist in the elastic parameters between CBM reservoirs and cap rocks and thus, there are difficulties in the application of an AVO inversion to a CBM reservoir. Consequently, the reflection coefficients of the upper interface of a CBM reservoir are calculated by the approximation equation and Zoeppritz equation, respectively. The elastic parameters for the calculation are the typical values of the CBM reservoir and cap rocks:

$V_{p1} = 3200$  m/s,  $V_{s1} = 1585$  m/s,  $\rho_1 = 2340$  kg/m<sup>3</sup>;  $V_{p2} = 1960$  m/s,  $V_{s2} = 1090$  m/s,  $\rho_2 = 1390$  kg/m<sup>3</sup>. As illustrated in Fig. 2, the error between the approximation equation and Zoeppritz equation is only 7% when the incidence angle is up to 30°. Furthermore, the classification of CBM using AVO abnormality operated by Chen et al. (2014) and AVO attribute inversion for crack characteristics conducted by Peng et al. (2005), verified the better applicability for incidence angles of < 30°. Thus, it is reasonable to consider that this approximation equation is acceptable for use with CBM reservoirs where the incidence angle is < 30°.

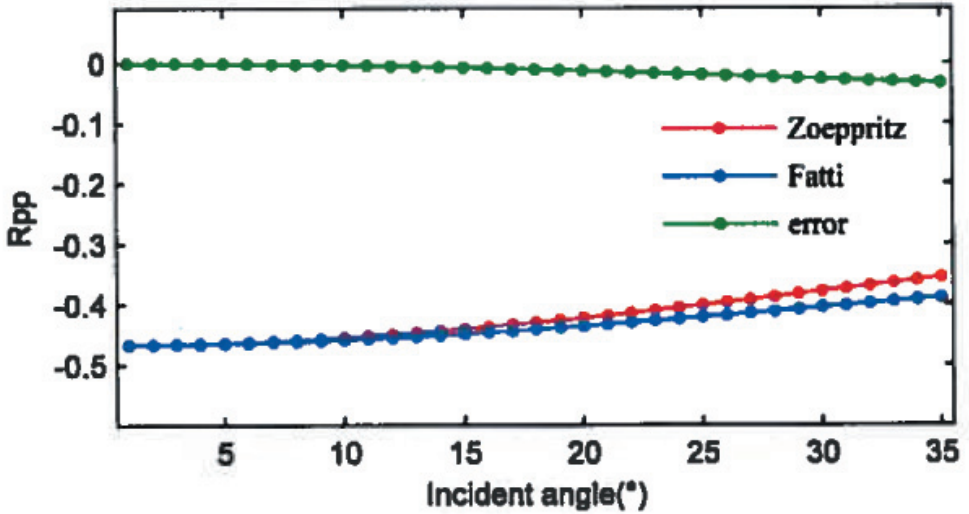


Fig. 2. R<sub>pp</sub> values calculated using the Zoeppritz equation and approximation equation.

**Inversion model establishment**

Rewriting eq. (1) in matrix form means that the convolution model of pre-stack gathers can be expressed as follows:

$$d = w * [A(\theta)m] = G(\theta)m \quad , \quad (2)$$

where w is the wavelet (such as the Ricker wavelet and the well wavelet used in this paper),

$$m = [(\Delta I_p/2I_p) \quad (\Delta I_s/2I_s) \quad (\Delta \rho/2\rho)]^T$$

is the inversion reflection coefficients matrix,

$$A(\theta) = [1 + \tan^2\theta \quad -8(V_s/V_p)^2\sin^2\theta \quad -\tan^2\theta + 4(V_s/V_p)^2\sin^2\theta]$$

is the coefficients matrix, and G(θ) is the joint matrix of the wavelets and coefficients. Generally, the obvious correlation between the inversion coefficients affects the stability and precision of the inversion; therefore, their elimination by adopting a covariance matrix is necessary, which is shown in the Appendix (Zong et al., 2012, 2013). The convolution model after the elimination can be rewritten as follows:

$$d = G(\theta)'m' \quad . \quad (3)$$

## Bayes' theorem

The relationship between the a posteriori probability density function  $P(m'|d)$  and the a priori distribution  $P(m')$ , as well as the likelihood function  $P(d|m')$  about the inversion coefficients  $m'$ , is provided by Bayes' theorem, which can be written as follows:

$$P(m'|d) = P(m')P(d|m') / \int P(m')P(d|m')dm' \propto P(m')P(d|m') . \quad (4)$$

Generally, we estimate the optimal solution accomplished by the maximum a posteriori probability (MAP) (Downton, 2005). In eq. (4), the a priori distribution, including the correlation information of the inversion parameters, was used to construct the regularization term, for which there are many different choices, such as the Cauchy distribution, Huber distribution, and Gauss distribution. The modified Cauchy distribution is preferred as the a priori distribution, for the long tail distribution and non-consistent weighted coefficients, which lead to an obvious Sparse-spike effect for the inversion results (Zhang et al., 2013), as is shown in eq. (5):

$$P(m') = [1/(\pi\sigma_m)^M] \prod_{i=1}^M \exp\left\{-\frac{[(m'_i - \bar{m}')^2/\sigma_m^2]}{[1 + (m'_i - \bar{m}')^2/\sigma_m^2]}\right\} , \quad (5)$$

where  $\bar{m}'$  is the average of the uncorrelated inversion coefficients,  $\sigma_m$  is the standard deviation of uncorrelated inversion coefficients, and  $M$  is the number of sample points of inversion data. Generally, the Gaussian distribution is defined as the likelihood function, which describes the difference between the synthetic seismograms and the real seismic data. Its probability density function is shown in eq. (6):

$$P(d|m') = [1/(\sigma_n\sqrt{2\pi})] \exp\left\{-[d - G(\theta)'m']^2/2\sigma_n^2\right\} , \quad (6)$$

where  $\sigma_n$  is the standard deviation of noise. The combination of eqs. (5) and (6) means that the a posteriori probability density function can be written as follows:

$$P(m'|d) \propto \prod_{i=1}^M \exp\left\{-\frac{[(m'_i - \bar{m}')^2/\sigma_m^2]}{[1 + (m'_i - \bar{m}')^2/\sigma_m^2]}\right\} \\ \times \exp\left\{-[d - G(\theta)'m']^2/2\sigma_n^2\right\} . \quad (7)$$

The objective function  $F$  can be obtained after taking the log of eq. (7):

$$F(m') = [d - G(\theta)'m']^2 + 2\sigma_n^2 \sum_{i=1}^M \left\{ -[(m'_i - \bar{m}')^2 / \sigma_m^2] / [1 + (m'_i - \bar{m}')^2 / \sigma_m^2] \right\} . \quad (8)$$

Thereafter, based on the derivation of eq. (8), the inversion equation can be determined as follows:

$$[G(\theta)'^T G(\theta)' + \mu Q(m')]m' = G(\theta)'^T d , \quad (9)$$

where  $\mu = 2\sigma_n^2 / 2\sigma_m^2$  and  $Q(m') = 1/[1 + (m'_i - \bar{m}')^2 / \sigma_m^2]^2$  are both diagonal matrices. The term  $\mu Q(m')$  is the regularization term. Because of unpredictable and inevitable noise in the seismic data, AVO inversion problems need to be regularized. Accordingly, in the inversion process, the term can preserve the more reliable parameters by assigning larger weighting factors (Ma and Geng, 2013). However, for correlation with the inversion coefficient in the inversion equation (9), the equation becomes nonlinear and therefore, an iterative re-weighted least squares (IRLS) algorithm is adopted to solve it (Alemie, 2010, 2011). The solving procedure contains two iterative loops: the inner loop that is solved using the Fletcher-Reeves conjugate gradient algorithm (FR-CG) (Alemie, 2011), which means the conjugate gradient coefficient is calculated by the Fletcher-Reeves formula, and the outer loop based on updating the  $m'$  and  $\mu Q(m')$  (Downton et al., 2004, 2005). Generally, a reasonable solution can be obtained through five iterations.

## MODEL INVERSION

Typical logging curves of a CBM reservoir were selected as the case study for this chapter. Fig. 3 shows the  $I_p$ ,  $I_s$ , and  $\rho$  curves, Fig. 4(a) shows the angle gather synthetic seismogram convolving with the Ricker wavelet whose dominant frequency is 50 Hz, and Fig. 4(b) presents a synthetic seismogram containing Gaussian white noise with an S/N ratio equal to two. Their inversion results are shown in Figs. 5 and 6, respectively.

Without noise contained in the synthetic seismogram, as shown in Fig. 5, the inversion values of  $I_p$  and  $I_s$  are accurate at the location of the CBM reservoir (red area in Fig. 3), while the  $\rho$  values deviate slightly from the initial curves. There is a better match between the inversion curves and initial curves shown in Fig. 6, especially at the reservoir location, which means that there is less impact on  $I_p$ ,  $I_s$ , and  $\rho$  induced by the noise. It also illustrates that the introduction of the regularization term effectively suppresses the interference from noise, which leads to the accurate results from the inversion.

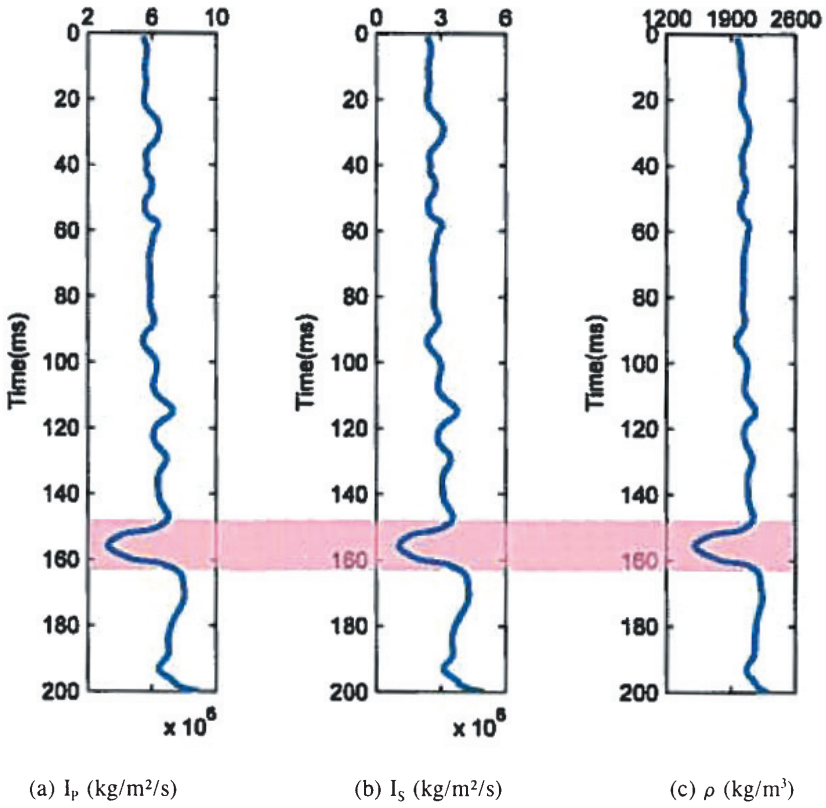


Fig. 3. Typical logging curves of a CBM reservoir.

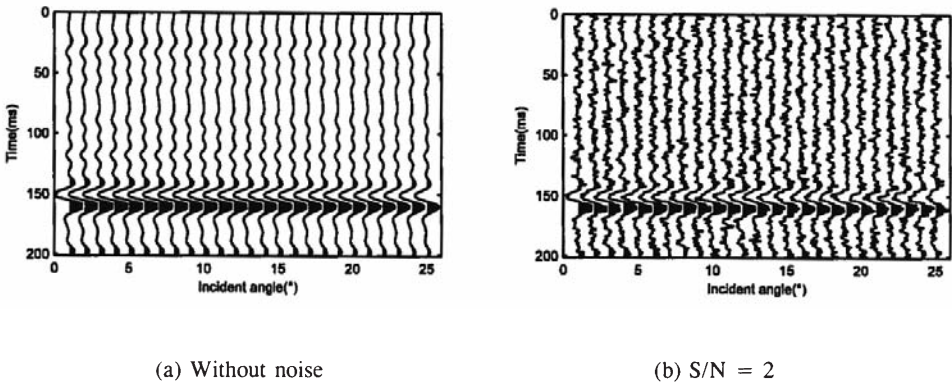


Fig. 4. Synthetic seismograms.



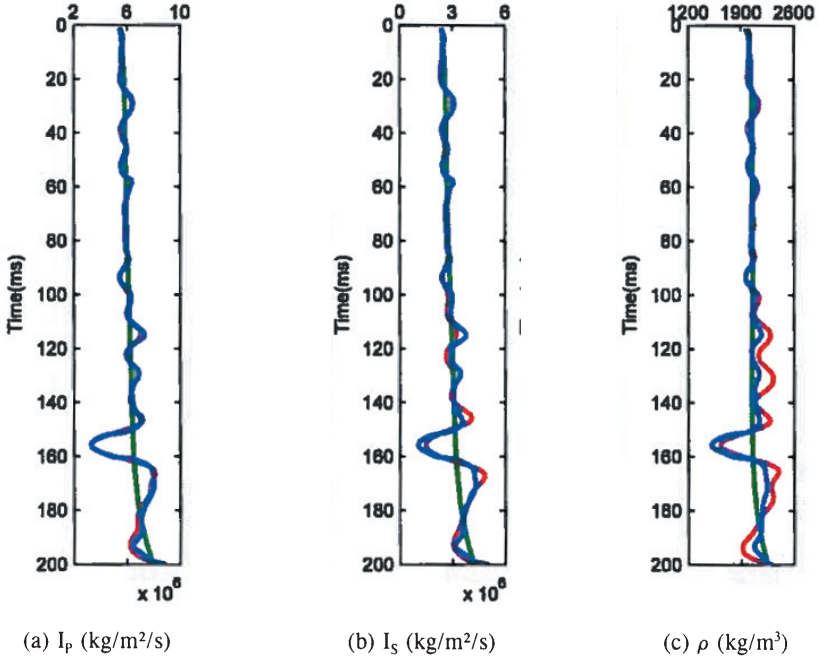


Fig. 5. Inversion results of synthetic seismogram without noise (red: inversion result, blue: real curves, green: original curves).

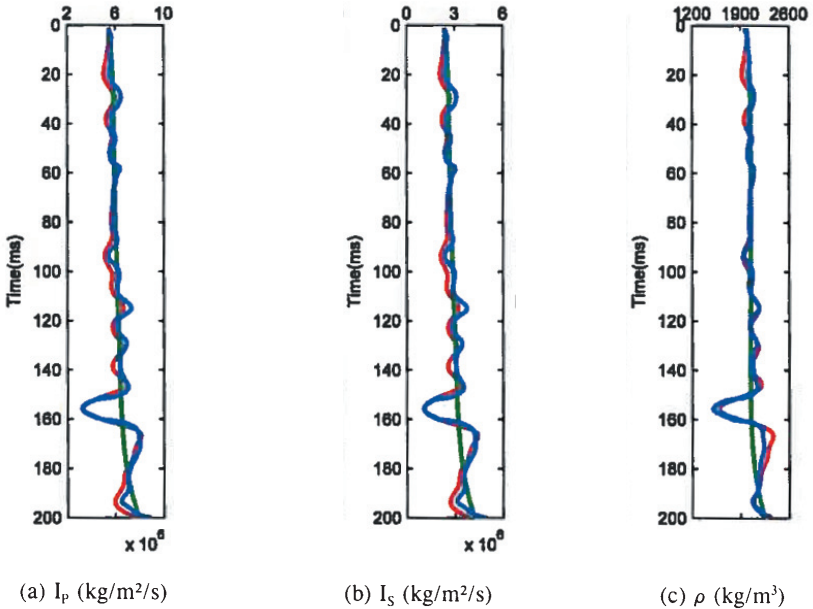


Fig. 6. Inversion results of synthetic seismogram with  $S/N = 2$  (red: inversion result, blue: real curves, green: original curves).

## A CASE STUDY

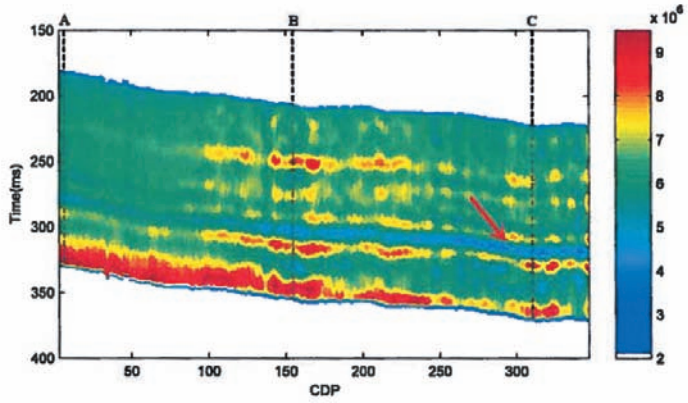
A through-well seismic profile, obtained from a field in Qinshui Basin, was examined to assess the applicability of the method to an actual CBM mining area and to attempt to distinguish areas of mylonitized coal development. There are about 350 CDP units in the object profile with 8 angle gathers from 5°-25° (i.e., 5°, 8°, 11°, 13°, 16°, 19°, 22°, and 24°) in every CDP. The objective reservoir, located at 280-320 ms, has a complete mudstone cap rock and its coal quality is grance anthracite. The tuning effect variance can be ignored because of the almost invariable thickness (about 4.7 m) of the reservoir. Three CBM wells are located in this profile, but only two (wells A and C) are used to establish the initial model; the third (well B) is used as a cross-validation well. The inversion results are exhibited in Fig. 7.

An area of low values can be recognized easily between 280 and 320 ms in the profiles of  $I_p$ ,  $I_s$ , and  $\rho$ , clearly indicating the location of the objective CBM reservoir (Fig. 7). The curves from well B, shown in Fig. 8, provide the validation of the inversion results. It can be seen that there is good agreement between the inversion curves and initial curves of  $I_p$  and  $I_s$ , as well as an accurate and acceptable inversion value at about 300 ms for the reservoir. However, a higher value of  $\rho$  is observed compared with the initial curve, even though there is a consistent variation tendency. Consequently, mapping out of the coal structure types by adopting  $I_p$  and  $I_s$  should be acceptable and reasonable, as illustrated by the cross validation. In Fig. 7(a) and 7(b), the red arrows indicate the low values of  $I_p$  and  $I_s$  compared with other areas of the objective reservoir, indicating areas with a relatively higher percentage of mylonitized coal.

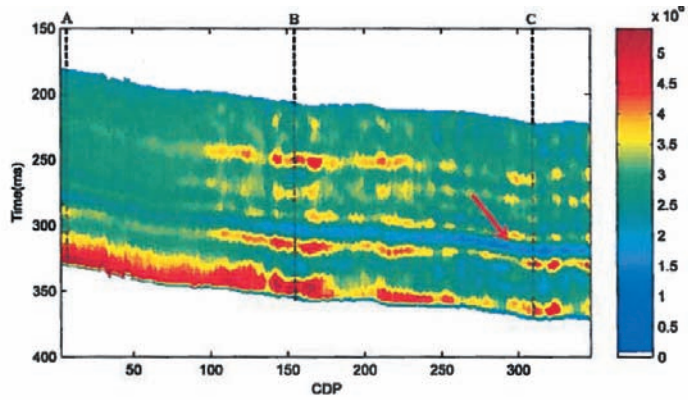
## CONCLUSIONS

In this study, we attempted to divide coal structure types and to delineate areas of mylonitized coal development within a CBM reservoir, based on pre-stack AVO simultaneous inversion results. The findings and conclusions are summarized as follows.

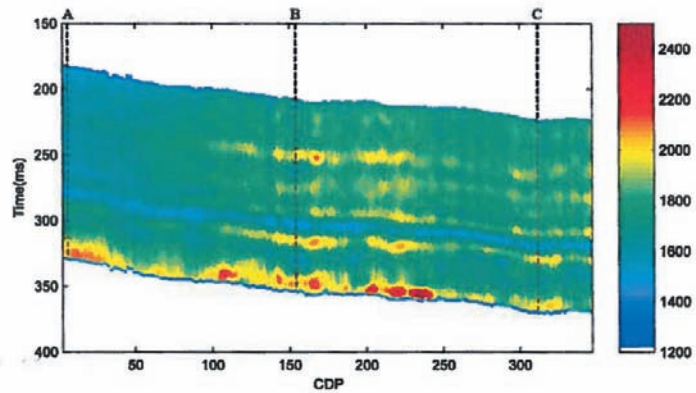
Coal structure is the principal factor controlling CBM enrichment in a field that has almost uniform characteristics such as reservoir thickness, cap rock, coal quality, and other geological conditions. Areas of mylonitized coal development showing abnormally low values of P-wave and S-wave impedance ( $I_p$  and  $I_s$ ) provide the theoretical basis for the method, and the possibility for the division of coal structure types and further division of CBM-enriched areas. The AVO approximation equation of Zoeppritz is acceptable for application to CBM reservoirs with small incidence angles (<30°). Values of  $I_p$  and  $I_s$  for a



(a)  $I_p$  (kg/m<sup>2</sup>/s)



(b)  $I_s$  (kg/m<sup>2</sup>/s)



(c)  $\rho$  (kg/m<sup>3</sup>)

Fig. 7. Inversion results of the seismic profile.

model with a low S/N ratio and seismic profile can be inverted by adopting a pre-stack AVO simultaneous inversion based on Bayes' theorem with a modified Cauchy distribution. Thereafter, based on the inversion results of  $I_p$  and  $I_s$ , areas of mylonitized coal development can be delineated.

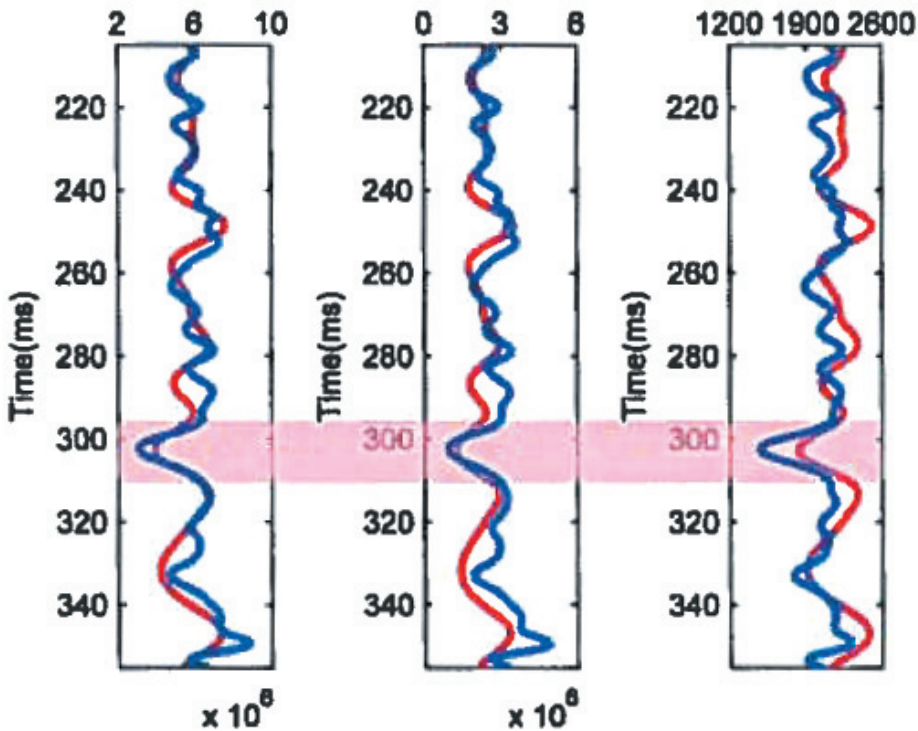
(a)  $I_p$  (kg/m<sup>2</sup>/s)(b)  $I_s$  (kg/m<sup>2</sup>/s)(c)  $\rho$  (kg/m<sup>3</sup>)

Fig. 8. Inversion results of well B (red: inversion result, blue: real curves).

## ACKNOWLEDGEMENTS

We would like to acknowledge the A Project Funded by the Priority Academic Program Development of Jiangsu Higher Education Institutions (PAPD), Innovation Training Project for Graduate Student of Jiangsu Province (No. KYLX 1399), and Fundamental Research Funds for the Central Universities (No. 2012QNA62) for funding this research. We also thank the anonymous reviewers for their constructive suggestions.

## REFERENCES

- Alemie, W., 2010. Regularization of the AVO inverse problem by means of a multivariate Cauchy probability distribution. M.Sc. thesis, University of Alberta, Edmonton.
- Alemie, W. and Sacchi, M.D., 2011. High-resolution three-term AVO inversion by means of a Trivariate Cauchy probability distribution. *Geophysics*, 76(3): R43-R55.
- Buland, A. and Omre, H., 2003. Bayesian linearized AVO inversion. *Geophysics*, 68(1): 185-198.
- Chen, X.P., Huo, Q.M., Lin, J.D., Wang, Y., Sun, F.J., Li, W.Z. and Li, G.Z., 2013. The inverse correlations between methane content and elastic parameters of coal-bed methane reservoirs. *Geophysics*, 78(4): D237-D248.
- Chen, X.P., Huo, Q.M., Lin, J.D., Wang, Y., Sun, F.J., Li, W.Z. and Li, G.Z., 2014. Theory of CBM AVO: 1. Characteristics of anomaly and why it is so. *Geophysics*, 79(2): D55-D65.
- Downton, J.E. and Lines, L.R., 2004. Three term AVO waveform inversion. Expanded Abstr., 74th Ann. Internat. SEG Mtg., Denver, 23: 215-218.
- Downton, J.E., 2005. Seismic parameter estimation from AVO inversion. Ph.D. thesis, University of Calgary, Calgary.
- Fatti, J.L., Smith, G.C., Vail, P.J., Strauss, P.J. and Levitt, P.R., 1994. Detection of gas in sandstone reservoirs using avo analysis: A 3-D seismic case history using the Geostack technique. *Geophysics*, 59: 1362-1376.
- Fu, X.H., Qin, Y. and Wei, Z.T., 2007. Coal-bed Methane Geology. China University of Mining and Technology Press, Xuzhou.
- Li, J.J., Cui, R.F., Pan, D.M., Chen, S.E., Hu, M.S. and Zhao, X., 2013. Prediction of gas outburst in a coalmine based on simultaneous prestack seismic inversion: a case study in China. *J. Seismic Explor.*, 22: 463-475.
- Ma, J.Q. and Geng, J.H., Cauchy prior distribution-based AVO elastic parameter estimation via weakly nonlinear waveform inversion. *Appl. Geophys.*, 2013, 10: 442-452.
- Peng, S.P., Gao, Y.F., Yang, R.Z., Chen, H.Q. and Chen, X.P., 2005. Theory and application of AVO for detection of coal-bed methane-A case from the Huainan coal-field. *Chin. J. Geophys.* (in Chinese), 48: 1475-1486.
- Peng, S.P., Chen, H.J., Yang, R.Z., Gao, Y.F. and Chen, X.P., 2006. Factors facilitating or limiting the use of AVO for coal-bed methane. *Geophysics*, 71(4): C49-C56.
- Qi, X.M. and Zhang, S.C., 2012. Application of seismic multi-attribute fusion method based on D-S evidence theory in prediction of CBM-enriched area. *Appl. Geophys.*, 9: 80-86.
- Wang, X., 2012. Research on prediction method by seismic attributes for high-risk coal of coal and gas outburst. Ph.D. thesis, China Univ. of Mining and Technology, Qingdao.
- Zhang, F.Q., Wei, F.J., Wang, Y.C., Wang, W.J. and Li, Y., 2013. Generalized linear AVO inversion with the priori constraint of trivariate Cauchy distribution based on Zoeppritz equation. *Chin. J. Geophys.* (in Chinese), 56: 2098-2115.
- Zong, Z., Yin, X. and Wu, G., 2012. AVO inversion and poroelasticity with P- and S-wave moduli. *Geophysics*, 77(6): N17-N24.
- Zong, Z., 2013. Methodologies of model driven inversion with pre-stack seismic data. Ph.D. thesis, China Univ. of Petroleum, Huadong.